Human Molecular Genetics, 2010, Vol. 19, No. 24 ***4871–4885***
doi:10.1093/hmg/ddq420
Advance Access published on September 27, 2010

Correction of CNS defects in the MPSII mouse model via systemic enzyme replacement therapy

Vinicia Assunta Polito[1,2], Serena Abbondante[1,2], Roman S. Polishchuk[1,3], Edoardo Nusco[1], Rosaria Salvia[1,2] and Maria Pia Cosma[1,2,4,*]

[1]Telethon Institute of Genetics and Medicine (TIGEM), and [2]Institute of Genetics and Biophysics (IGB), CNR, via P. Castellino 111, Naples 80131, Italy, [3]Consorzio Mario Negri Sud, via Nazionale, 8, Santa Maria Imbaro (CH) 66030, Italy and [4]Center for Genomic Regulation (CRG) and Institució Catalana de Recerca i Estudis Avançats (ICREA), c/Aiguader, 88, Barcelona 08003, Spain

Received August 3, 2010; Revised and Accepted September 20, 2010

Mucopolysaccharidosis type II (MPSII), or Hunter syndrome, is a devastating disorder associated with a shortened life expectancy. Patients affected by MPSII have a variety of symptoms that affect all organs of the body and may include progressive cognitive impairment. MPSII is due to inactivity of the enzyme iduronate-2-sulfatase (IDS), which results in the accumulation of storage material in the lysosomes, such as dermatan and heparan sulfates, with consequent cell degeneration in all tissues including, in the severe phenotype, neurodegeneration in the central nervous system (CNS). To date, the only treatment available is systemic infusion of IDS, which ameliorates exclusively certain visceral defects. Therefore, it is important to simultaneously treat the visceral and CNS defects of the MPSII patients. Here, we have developed enzyme replacement therapy (ERT) protocols in a mouse model that allow the IDS to reach the brain, with the substantial correction of the CNS phenotype and of the neurobehavioral features. Treatments were beneficial even in adult and old MPSII mice, using relatively low doses of infused IDS over long intervals. This study demonstrates that CNS defects of MPSII mice can be treated by systemic ERT, providing the potential for development of an effective treatment for MPSII patients.

INTRODUCTION

The enzyme iduronate-2-sulfatase (IDS) removes the sulfate group from the glycosaminoglycans (GAGs), dermatan and heparan sulfates, and its absence or inactivity results in mucopolysaccharidosis type II (MPSII), or Hunter syndrome, a lysosomal storage disorder. The pathogenetic mechanisms at the basis of MPSII are still unknown. The block in the catabolic pathway of derman and heparan sulfates results in the accumulation of undegraded substrates in the cells and tissues of MPSII patients, with progressive cellular vacuolization and cell death (1,2). MPSII occurs in both mild and severe forms, which cover a broad spectrum of symptoms, such as dysmorphic facial features, hepatosplenomegaly, skeletal deformities, joint stiffness, severe retinal degeneration, hearing impairmentand, in the severe phenotype, a progressive deterioration of the central nervous system (CNS). The incidence of MPSII has been estimated at around one affected male in 162 000 live births (3–5). This absence or inactivity of IDS has been shown to be due to point mutations or deletions in the *IDS* gene, which maps on the X chromosome (6–10). The severe form of MPSII is characterized by progressive somatic and neurological involvement, and the onset of the disease usually occurs between the second and fourth year of age. Death generally occurs between the age of 10 and 14 years, and it is generally due to cardiac failure or airway obstruction (1,2).

The MPSII ($Ids^{y/-}$) mouse model shows the features of Hunter syndrome. No IDS activity can be detected in any of its tissues, and the affected mice show progressive accumulation of GAGs in all of their organs, along with

*To whom correspondence should be addressed. Tel: +34 933160370; Fax: +34 933160099; Email: pia.cosma@crg.es

neuropathological defects. The onset of this phenotype is at 3–4 months of age, and it becomes progressively severe through adult life (11,12).

We have thoroughly characterized the CNS phenotype of the MPSII mouse model, where diffuse neurodegeneration is seen in different CNS areas such as reduced neuronal density, increased ubiquitination, severe gliosis and increased apoptosis; this phenotype becomes more severe with disease progression through life. The mice also show progressive degeneration of Purkinje cell neurons in the cerebellum (13).

Recently, we established an efficient gene-therapy approach to treat both the visceral and CNS defects in these MPSII mice. MPSII pups injected with the adeno-associated viral serotype 2/5 vector carrying human IDS cDNA showed full correction of the CNS symptoms and the visceral defects for up to 18 months after therapy. Furthermore, we demonstrated that the CNS rescue was due to the crossing of the blood–brain barrier by the IDS enzyme (13).

Enzyme replacement therapy (ERT) with recombinant human proteins has been used successfully in the treatment of some other lysosomal storage diseases such as Gaucher disease (14,15), Fabry disease (16–18), MPSI (19,20), MPSVI (21,22) and Pompe disease (23) and there are also some ongoing trials for Niemann–Pick type B (24). In addition, ERT at high doses in mouse models of α-mannosidosis, or MPSVII, and metachromatic leukodystrophy leads to enzyme delivery across the blood–brain barrier, thereby partially reversing the storage in brain tissues (25–27). The human IDS enzyme (Elaprase® [idursulfase], Shire Human Genetic Therapies, Inc.) is already available commercially in many countries for the treatment of MPSII and ameliorates certain visceral defects (28–30); however, idursulfase does not ameliorate the CNS defects in these MPSII patients. Prior to the availability of idursulfase, the treatment of patients with MPSII was palliative and focused on the management of the clinical problems.

Both cognitive and neurological impairment is a devastating problem for patients affected by the severe form of MPSII. Many obstacles need to be overcome to develop a therapy to treat the CNS defects of MPSII patients; however, the quality of life of these patients would greatly benefit by the simultaneous treatment of their systemic and CNS defects. Up to now, ERTs have been largely inefficient to treat CNS phenotype in patients affected by lysosomal storage disorders, and this was mainly due to the presence of the blood–brain barrier and to the fast clearance of the infused enzymes from the blood.

In the present study, we demonstrate that systemic administration of human IDS to MPSII mice via ERT allows the enzyme to clear the GAG storage in the brain, to correct many of the neurodegeneration markers and to rescue the neurobehavioral CNS disease phenotype. Through ERT, we can strongly ameliorate the CNS defects, even when using a relatively low dose of IDS, and with both short and prolonged treatment times. Furthermore, we show the rescue of the CNS defects even in a group of old (aged 7 months and treated for 3 months) MPSII mice. These data open up hope for the treatment of MPSII patients exhibiting cognitive impairment.

RESULTS

IDS activity can be partially rescued in the brains of MPSII mice after ERT

ERT is the current approach to treat MPSII patients. To investigate whether systemic application of IDS enzyme via ERT can deliver enzyme to the brain and therefore prevent or cure the CNS degeneration, we implemented different therapeutic approaches. These were designed to identify the minimal IDS dose and the longest treatment-interval time sufficient to treat the CNS phenotype of MPSII mice. Thus we proceeded as follows.

(A) A group of adult MPSII mice (aged 2 months; $n = 21$; seven mice per group) received human IDS doses of 10, 5 or 1.2 mg/kg in a volume of 300 μl via the tail vein, every other day (1–2), for a total period of 1 month. Groups of untreated, age-matched, MPSII ($n = 5$) and wild-type ($n = 5$) mice were used as controls.

(B) A group of adult MPSII mice (aged 2 months; $n = 14$; seven mice per group) received human IDS doses of 1.2 mg/kg in a volume of 300 μl via the tail vein, once every 4 days (1–4) and once every 7 days (1–7), for a total period of 1 month. Groups of untreated, age-matched, MPSII ($n = 5$) and wild-type ($n = 5$) mice were used as controls.

(C) A group of old MPSII mice (aged 7 months; $n = 21$; seven mice per group) received human IDS doses of 10 mg/kg in a volume of 300 μl via the tail vein, every other day (1–2), once every 4 days (1–4) and once every 7 days (1–7), for a total period of 3 months. Groups of untreated, age-matched, MPSII ($n = 5$) and wild-type ($n = 5$) mice were used as controls.

(D) A group of adult MPSII mice (aged 3 months; $n = 4$) received human IDS doses of 1.2 mg/kg in a volume of 300 μl via the tail vein, once every 7 days (1–7), for the longer period of 7 months. Groups of untreated, age-matched, MPSII ($n = 5$) and wild-type ($n = 5$) mice were used as controls.

During these treatments, IDS activity was measured in the plasma of all of the treated mice, every other month from T1 to T7 (months 1, 3, 5 and 7), at 4 h after the last injection. The IDS plasma activity was extremely high and was even higher than the activity measured in the wild-type control mice. Interestingly, also with the group D mice that received IDS for the longest time, after 7 months their mean plasma IDS activity was 8.7-fold higher than that of the wild-type control mice (Table 1). Moreover, in all of the groups of mice, the IDS activity measured 48 h after each injection was higher (from 4- to 11-fold, depending on treatments) than the levels in the untreated MPSII mice, but was also comparable to levels measured in the untreated wild-type mice (Table 2). These plasma IDS activities returned to the levels measured in the untreated MPSII mice 72 h after the last injections of each treatment protocol (data not shown). These data clearly show that the IDS enzyme is very stable, showing slow plasma clearance; indeed, it remains at high levels in the blood of the treated mice for a long time.

The treated mice (groups A–D) were then sacrificed at different times 4 h after the final administration of IDS of

Table 1. Plasma IDS activities according to mouse treatment groups, 4 h after last treatment

Mouse treatment groups (treatment schedule; *n*)	Sampling time for plasma IDS activity (nmol/4 h/mg protein)			
	T1	T3	T5	T7
Controls				
Wild-type (untreated; 5)	350 ± 16.0	261 ± 14.0	233 ± 23.0	221 ± 11.0
MPSII (untreated; 5)	18 ± 0.5	16 ± 0.8	21 ± 0.9	19 ± 1.2
Group A				
MPSII + 10 mg/kg IDS (1–2; 7)	10938 ± 779			
MPSII + 5.0 mg/kg IDS (1–2; 7)	7500 ± 447			
MPSII + 1.2 mg/kg IDS (1–2; 7)	2790 ± 226			
Group B				
MPSII + 1.2 mg/kg IDS (1–4; 7)	1810 ± 151			
MPSII + 1.2 mg/kg IDS (1–7; 7)	1877 ± 136			
Group C				
MPSII + 10 mg/kg IDS (1–2; 7)	9292 ± 611	6957 ± 557		
MPSII + 10 mg/kg IDS (1–4; 7)	7471 ± 118	6459 ± 301		
MPSII + 10 mg/kg IDS (1–7; 7)	6642 ± 389	6633 ± 390		
Group D				
MPSII + 1.2 mg/kg IDS (1–7; 4)	2828 ± 198	2551 ± 215	2212 ± 26	1724 ± 193

Table 2. Plasma IDS activities according to mouse treatment groups, 48 h after last treatment

Mouse treatment groups (treatment schedule; *n*)	Sampling time for plasma IDS activity (nmol/4 h/mg protein)			
	T1	T3	T5	T7
Controls				
Wild-type (untreated; 5)	350 ± 16.0	261 ± 14.0	233 ± 23.0	221 ± 11.0
MPSII (untreated; 5)	18 ± 0.5	16 ± 0.8	21 ± 0.9	19 ± 1.2
Group A				
MPSII + 10 mg/kg IDS (1–2; 7)	271 ± 74			
MPSII + 5.0 mg/kg IDS (1–2; 7)	296 ± 54			
MPSII + 1.2 mg/kg IDS (1–2; 7)	217 ± 38			
Group B				
MPSII + 1.2 mg/kg IDS (1–4; 7)	105 ± 27			
MPSII + 1.2 mg/kg IDS (1–7; 7)	116 ± 46			
Group C				
MPSII + 10 mg/kg IDS (1–2; 7)	208 ± 11	192 ± 12		
MPSII + 10 mg/kg IDS (1–4; 7)	204 ± 10	183 ± 10		
MPSII + 10 mg/kg IDS (1–7; 7)	210 ± 30	156 ± 37		
Group D				
MPSII + 1.2 mg/kg IDS (1–7; 4)	214 ± 90	216 ± 94	169 ± 46	159 ± 38

each treatment protocol. In parallel, the groups of untreated MPSII and untreated wild-type mice were also sacrificed. The IDS activities were measured in homogenates from their brains and visceral tissues.

Group A showed brain IDS activities that decreased in parallel with the concentrations of IDS injected. Interestingly, with the administration of the lowest dose of IDS (1.2 mg/kg), some IDS activity was still detected in the brains of the treated MPSII mice (Fig. 1A). Surprisingly, the same IDS activities were detected in the group B mice, which received 1.2 mg/kg doses at longer time intervals, i.e. treatment every 4 and 7 days (Fig. 1B). The group C treatment showed that IDS can also be partially detected in MPSII mice of 7 months of age, even when these mice were treated once every 7 days (Fig. 1C). Finally, the MPSII mice in group D, which were treated with 1.2 mg/kg once every 7 days for a prolonged period of time, also showed some IDS activity in their brains (Fig. 1D).

In conclusion, in all groups of treated MPSII mice, and even in the adult MPSII mice treated with the lowest IDS dose (1.2 mg/kg) once every 7 days, the IDS activities measured in the brains were higher than those of the untreated MPSII mice. However, as expected, the IDS activities were much lower with respect to those measured in the wild-type mice.

We also tested the IDS enzyme activities in the homogenates from liver, kidney, lung, spleen, heart and skeletal muscle of the treated mice and the untreated MPSII and wild-type mice (groups A–D). The tissue IDS activities measured in the treated mice (for all three IDS concentrations injectedand for all of the intervals of time) were always higher than the activities measured in the untreated MPSII mice and were also higher, with few exceptions, than the activities measured in the visceral tissues of the wild-type mice (Supplementary Material, Fig. S1A–D).

Clearance of lysosomal GAG accumulation in the brains and tissues of the treated and control mice

Next, the brains and visceral tissues of the sacrificed mice were analyzed for GAG clearance by Alcian blue staining of

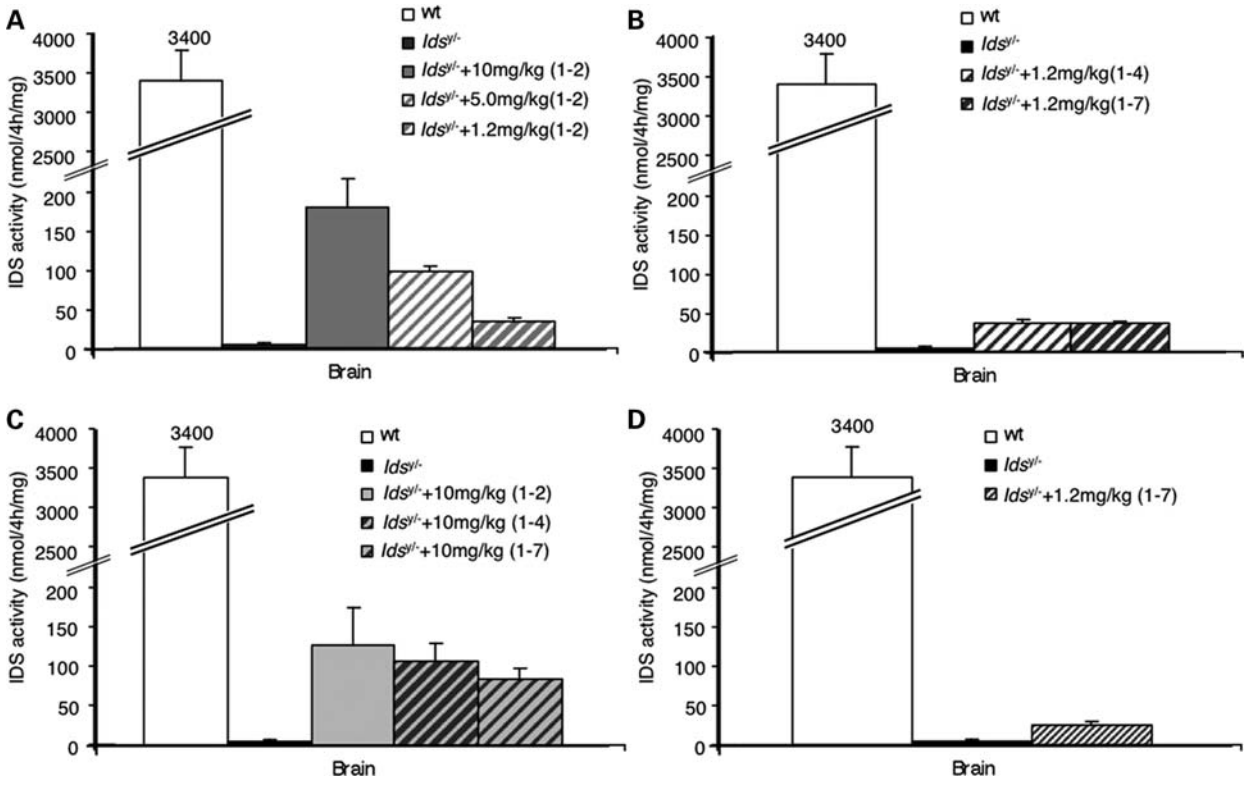

Figure 1. IDS activities following ERT, measured in brain homogenates of untreated wild-type (wt; $n = 5$) and MPSII (*Ids*$^{y/-}$; $n = 5$) mice and treated MPSII mice sacrificed 4 h after the final IDS treatments (as indicated). (**A**) Group A ($n = 7$); (**B**) group B ($n = 7$); (**C**) group C ($n = 7$); (**D**) group D ($n = 4$). See text for details. Data are means ± standard deviations. $P < 0.05$ versus untreated MPSII control (ANOVA test).

the treated and untreated MPSII and wild-type mice. There was almost total clearance of GAG accumulation in the choroid plexus of the third and fourth ventricles and in the cortex and thalamus of all of groups of mice, with respect to the untreated MPSII mice (Fig. 2). Of note, even with the low dose of IDS administered over the longer time interval (1.2 mg/kg once every 7 days), there was good clearance of GAGs in all of the regions of the brain analyzed. Furthermore, there was clearance of GAGs when the mice were treated not just for 7 months, but also for only 1 month.

These data show that GAGs can be cleared with both short and prolonged ERT protocols with a low dose of infused IDS in juvenile mice, and they can also be cleared in the older mice with higher doses of IDS infusion. Importantly, the GAGs were fully cleared in all of the visceral tissues (Supplementary Material, Fig. S2) and in the urine (Supplementary Material, Fig. S3) of all of the treated mice at all of the IDS concentrations infused and at all of the infusion time intervals.

IDS activity and GAG clearance in the brains and tissues of treated and control mice sacrificed 4 days after the final IDS infusion

We then wanted to determine whether we could measure IDS enzyme activity and GAG clearance after prolonged periods of time from the last IDS administration. Thus, to evaluate the residual IDS activity, a group of adult MPSII mice (aged 2 months; $n = 4$) were treated with 1.2 mg/kg IDS once every 7 days (group E) for 1 month, and 4 days after the final IDS injection, they were sacrificed. Groups of untreated, age-matched, MPSII and wild-type mice were used as controls.

Surprisingly, 4 days after the last IDS administration, we still detected IDS activity in both the brains and the tissues of the treated mice; in most organs (brain, liver, kidney and spleen), this activity was higher than that for the untreated MPSII mice (Fig. 3A and B). GAG clearance was also seen to persist in the different brain areas and in the visceral tissues of these treated mice (Fig. 3C and D).

These data show that the IDS activity remains in the brain and the tissues for a long time at sufficient levels to maintain the clearance of GAG accumulation. For this reason, the administration of IDS once every 7 days appears sufficient to correct both the brain and the tissue defects.

Partial correction of the brain defects in the treated MPSII mice

We have recently shown that progressive accumulation of GAGs in lysosomes of neurons leads to severe vacuolization. In addition, we have seen diffuse neurodegeneration in the thalamus, cerebral cortex and brain stem, according to reduced neuron densities (decreased anti-NeuN signals) and to increased ubiquitin-expressing neurons. This was also associated with the triggering of apoptosis, as shown by TUNEL-positive signals in neurons of the thalamus, cerebral cortex and brain stem of MPSII mice (13).

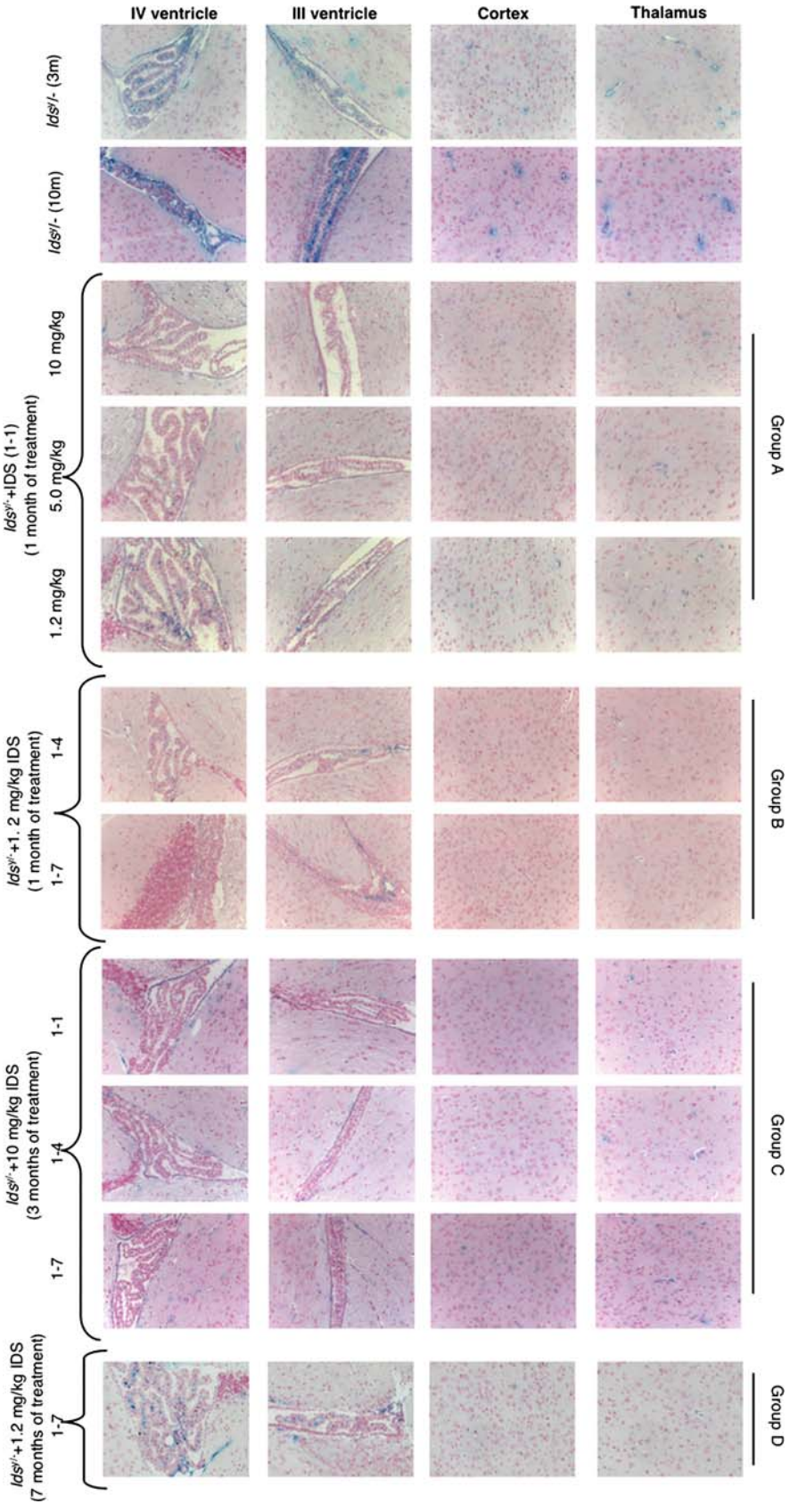

Figure 2. Representative GAG accumulation following ERT, measured by Alcian blue staining of sections of different brain regions of untreated MPSII ($Ids^{y/-}$) mice (3 and 10 months old) and groups A–D treated MPSII mice (as indicated). See text for details. Magnification, 20×.

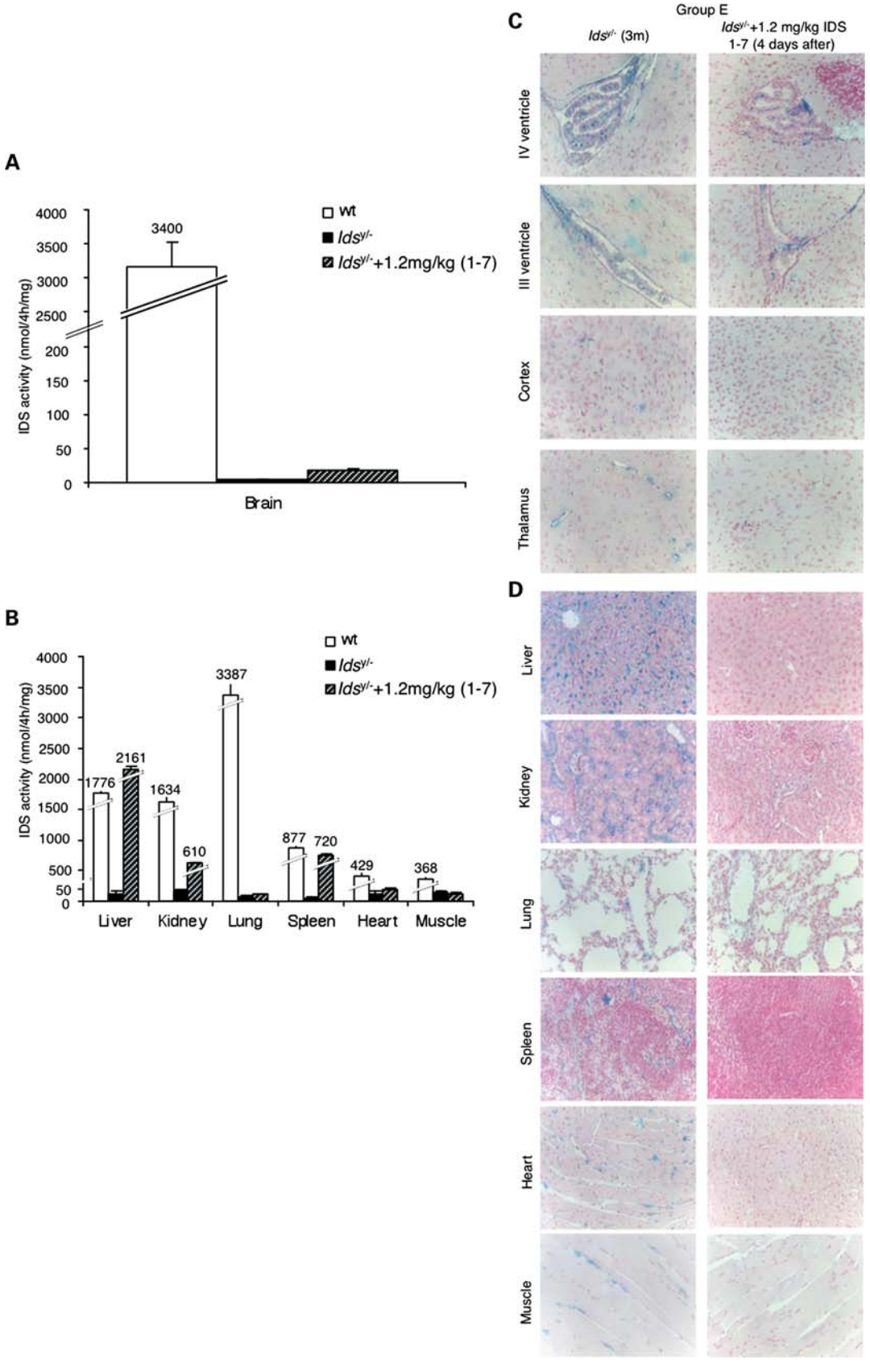

Figure 3. IDS activities and GAG accumulation following ERTin the brain and visceral tissue homogenates of 3-month-old mice sacrificed 4 days after the final IDS treatments. (**A** and **B**) IDS activities of untreated wild-type (wt; $n = 5$) and MPSII ($Ids^{y/-}$; $n = 5$) mice and treated MPSII mice (as indicated; $n = 4$). Data are means $\pm$ standard deviations. $P < 0.05$ versus untreated MPSII control (ANOVA test). (**C** and **D**) Representative GAG accumulation measured by Alcian blue staining of sections from untreated MPSII ($Ids^{y/-}$; 3 months old) mice and treated MPSII mice (as indicated) for different brain regions (C) and visceral tissues (D) (as indicated). Magnification, $20\times$.

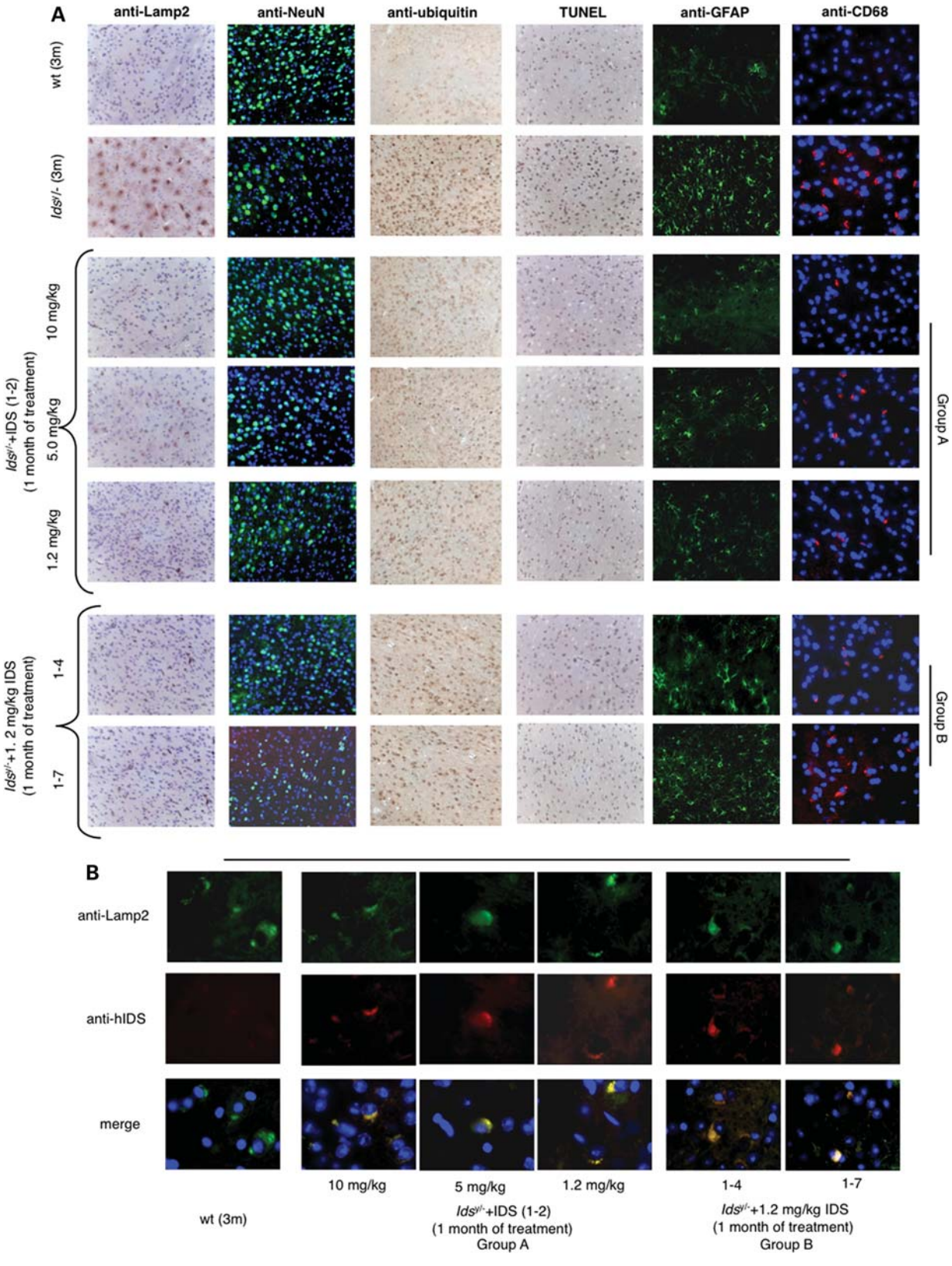

Figure 4. Representative analysis of the rescue of CNS markers in the thalamus following ERT, with untreated wild-type (wt; 3 months old; A and B) and MPSII (*Ids*$^{y/-}$; 3 months old, A) mice and treated MPSII mice (A and B) sacrificed 4 h after the final IDS treatments in groups A andB, as indicated. (**A**) Immunohistochemistry (IHC) and immunofluorescence (IF) monitored according to (left to right): anti-Lamp2 IHC for GAG storage; anti-NeuN IF for neuron density; anti-ubiquitin IHC for ubiquitination; TUNEL assay for apoptosis; anti-GFAP IF for gliosis (all magnification 20×) and anti-CD68 IF for macrophage infiltration (magnification, 40×). See text for details. (**B**) Co-localization of the lysosomal marker Lamp-2 (anti-Lamp2 antibody) and the IDS protein (anti-hIDS antibody) as seen in the merge, as indicated. Magnification, 100×.

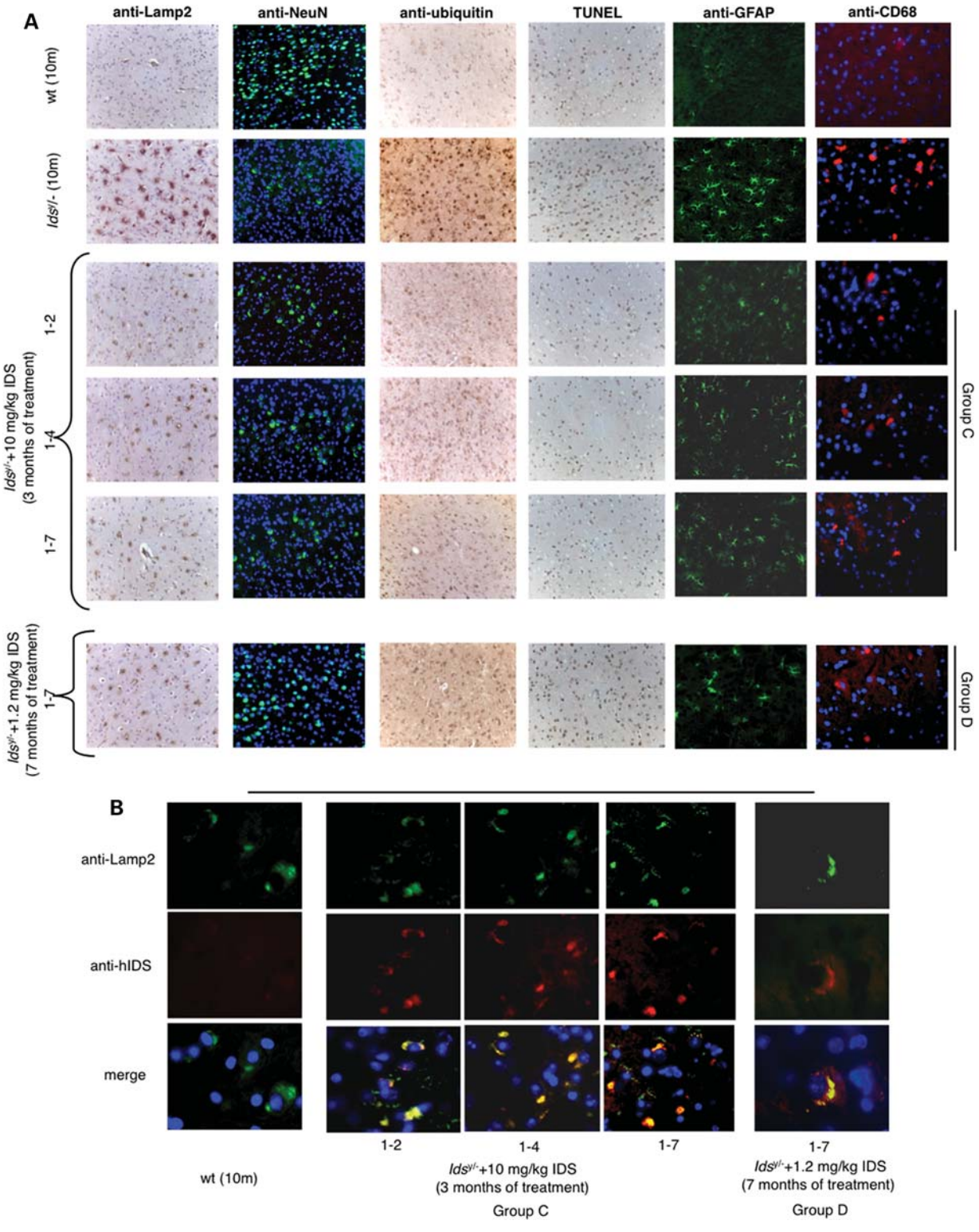

Figure 5. Representative analysis of the rescue of CNS markers in the thalamus following ERT, as for ×Figure 4, with untreated wild-type (wt; 10 months old; **A** and **B**) and MPSII (*Ids*$^{y/-}$; 10 months old, A) mice and treated MPSII mice (A and B) sacrificed 4 h after the final IDS treatments in groups **C** and **D**, as indicated. See legend to Figure 4 and text for details.

Here, we saw a clear reduction in the lysosomal GAG accumulation, as showed by the anti-Lamp2 immunostaining that marks the lysosome storage that is massively evident in the untreated MPSII mice (Figs 4A and 5A). A clear amelioration of neurodegeneration was also evident in the treated mice in all of the groups, as revealed by reductions in anti-ubiquitin

and TUNEL signals in neurons of the thalamus (Figs 4A and 5A) as well as in the cortex and brain stem (data not shown). Accordingly, we also noted increases in the neuron density (as anti-NeuN immunostaining) in the treated mice of groups A, B and D when compared with the untreated MPSII mice (Figs 4A and 5A).

As expected, there was only a small increase in the neuron density in the brains of mice of group C (Fig. 5A); indeed, the treatment of these mice of 7 months of age appeared to have been started too late, when the neurodegeneration was already too advanced.

MPSII mice also showed increased numbers of activated astrocytes, as revealed by anti-GFAP staining. This was clearly ameliorated in the thalamus, cortex and brain stem in all of the treated mice (Figs 4A and 5A; data not shown). We also analyzed the inflammatory responses in the thalamus, cortex and brain stem, by evaluating infiltration of activated macrophages, using an anti-CD68 antibody with tissue sections. The untreated MPSII mice showed high levels of inflammation; in contrast, the treated mice showed significant reductions in macrophage infiltration in all of the CNS areas analyzed (Figs 4A and 5A).

Together these data demonstrate that through ERT we can promote partial correction of the CNS defects; importantly, this holds true even for the treatment of the older mice. Indeed, these old mice (group C) showed clear amelioration of the marker phenotype even when treated once every 7 days. Importantly too, prolonged treatment (7 months treatment; group D) with a low dose of IDS (1.2 mg/kg) and with the longest interval between administrations (once every 7 days) also improved the CNS phenotype of these treated adult mice.

To confirm the presence of the IDS enzyme in the brains of these treated mice, we performed a co-immunostaining using anti-lamp2 and anti-human IDS antibodies with brain sections of MPSII treated mice belonging to all of the groups. We clearly saw labeling for IDS in the thalamus of the treated mice with all of the treatment protocols (Figs 4B and 5B).

Clearance of lysosome storage after ERT as evaluated by ultrastructural analysis

Ultrastructural analysis of thin sections from the cerebellum of wild-type mice revealed electron-dense membrane structures with morphological features of lysosomes in Purkinje cells (Fig. 6A). These lysosomal organelles were mainly electron-dense with a few translucent areas in the lumen, and they usually ranged from 300 to 1000 nm in diameter. In contrast, the cytoplasm of Purkinje cells from the MPSII mice contained large lysosome-like organelles (Fig. 6B), which in some cases reached even 3000 nm in diameter and were, on average, more than twice the diameter of those of the wild-type mice Purkinje cell lysosomes (Fig. 6D), as revealed by the morphometric analysis. The lumen of these organelles was filled with the heterogeneous material, part of which looks like 'fuzzy flakes' that resemble GAGs. Taken together, these ultrastructural features suggest that the degradation processes in these organelles are impaired, which results in GAG storage.

We analyzed the Purkinje cells of the group C treated mice (the oldest mice) by ultrastructural analysis and found significant improvement of the above-described MPSII phenotype. Indeed, for all the IDS treatments, the average diameters of the lysosome-like structures decreased (although they remained greater than that in the untreated wild-type mice; Fig. 6C and D). The overall population of the lysosomes was also highly variable in terms of the content. Some lysosomal organelles in the treated mice showed heterogeneous material in the lumen, as seen for the Purkinje cells from the untreated MPSII mice (Fig. 6C, black arrows), whereas others more resembled the electron-dense lysosomes for the Purkinje cells from the untreated wild-type mice (Fig. 6C, black arrowhead). All in all, the ultrastructural analysis confirms that the IDS cleared GAG storage in the lysosomes. Interestingly, this was also seen for the group of older mice that had the more severe GAG-storage phenotype.

Treated MPSII mice show improved sensorimotor coordination in the open-field and rotarod tests

The mice in groups C and D underwent both the open-field and rotarod tests. These neurobehavioral tests were carried out only in these two groups of mice because the clear phenotype measured by these two tests can be seen only in MPSII mice from about 5 to 6 months of age (11). The ability to explore, the locomotion and the anxiety to move of the treated mice were determined through the open-field test. As shown in Figure 7, the performance in the open-field test showed both the vertical and horizontal activities to be fully corrected in the treated mice and to be comparable to the untreated wild-type mice (Fig. 7A, B, D and E).

We have previously shown that MPSII mice undergo a loss of Purkinje cells in the cerebellum (11). The rotarod test evaluates the sensorimotor coordination and the rescue of these cerebellum defects in the treated mice. The treated mice significantly improved their performances when compared with the untreated MPSII mice; indeed, in both the groups of mice, the latency times of the treated mice were almost comparable to those of the untreated wild-type mice (Fig. 7C and F).

These data show that by systemic ERT, the MPSII CNS defects can also be functionally rescued, confirming the value of this therapeutic approach for the treatment of MPSII.

DISCUSSION

To date, the only therapy available to treat MPSII patients is ERT, which is only effective to ameliorate certain systemic defects. Progressive neurodegeneration in the severe form of MPSII patients is a devastating feature leading to dramatic intellectual impairment in the patients. It is therefore very important to establish an ERT protocol that can ameliorate the CNS symptoms in addition to the visceral phenotype of MPSII patients. At present, MPSII patients are treated with an infusion of 0.5 mg/kg recombinant human IDS once a week (28–30); here, we show that in juvenile mice, the systemically infused low dose of 1.2 mg/kg human IDS administered once every 7

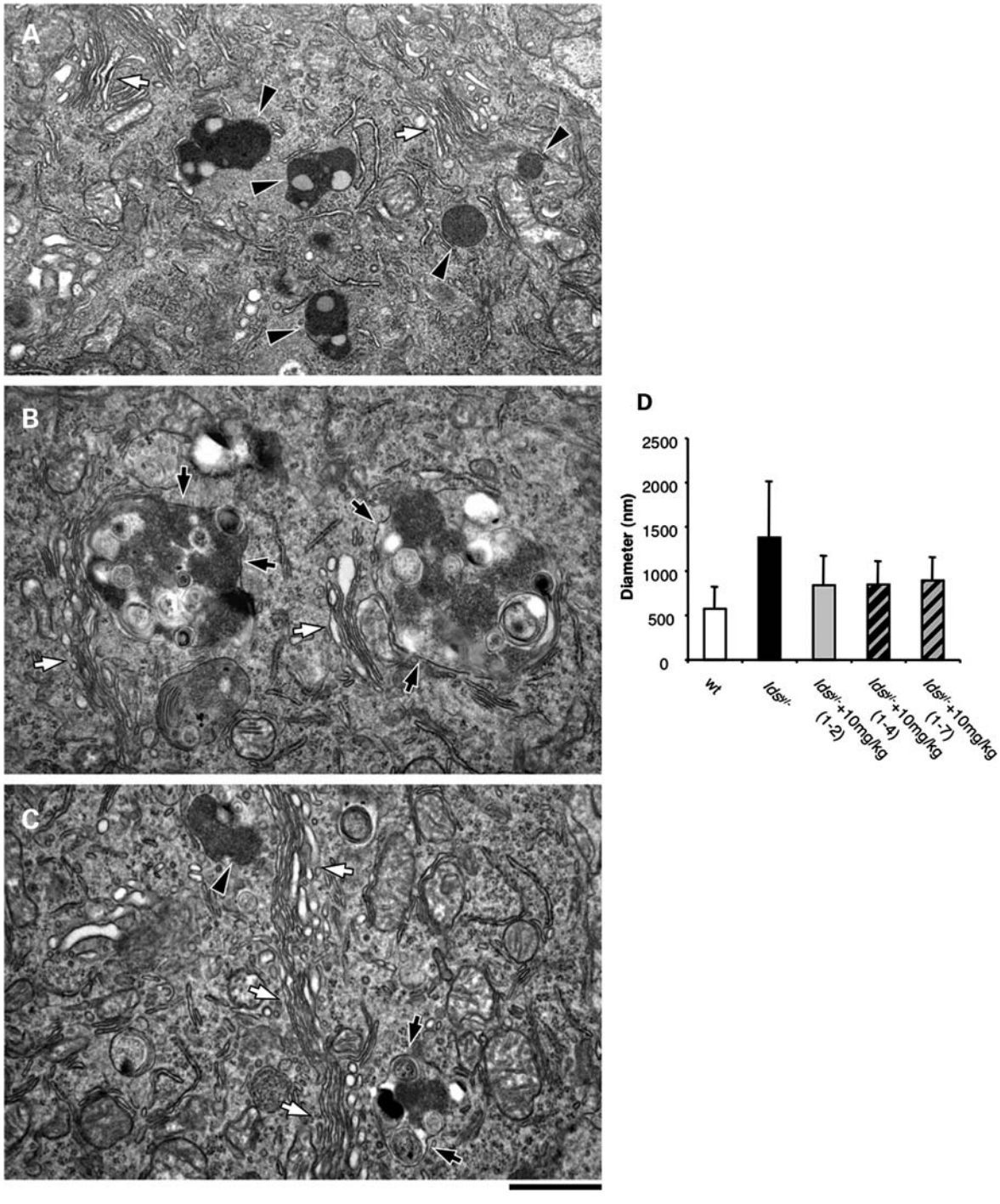

Figure 6. Representative analysis (**A**–**C**) and quantification (**D**) of the ultrastructure of the lysosome-like organelles in the Purkinje cells in thin sections of cerebellum from untreated wild-type (wt; A and D) and MPSII (*Ids*$^{y/-}$; B and D) mice and treated MPSII mice (C and D) sacrificed 4 h after the final IDS treatments in group C, as indicated. In all cases, the Purkinje cells were sectioned through their central area (judged on the basis of the presence of the Golgi membranes; A–C, white arrows) to ensure most representative sampling and analysis. (A) Black arrowheads, small electron-dense lysosome-like organelles. (B) Black arrows, large vacuolar structures containing heterogeneous material. (C) Black arrowheads, significantly smaller vacuolar structures containing heterogeneous material; black arrows, lysosomes with regular size and morphology were also detected. Scale bar, 1000 nm. (D) Quantification of the lysosome diameter (average $\pm$ SD, $n = 80$ lysosomes) in sections of treated MPSII and control mice as indicated. $P < 0.05$ versus untreated MPSII control (ANOVA test).

days for short and for prolonged treatment periods is sufficient to ameliorate and apparently prevent progression of the CNS defects in these MPSII mice. Thus one of the important observations of the present study is that as opposed to much higher doses of other enzymes needed for ERT (such as β-glucuronidase in MPSVII mice, arylsulfatase A in metachromatic leukodystrophy mice and α-mannosidase in α-mannosidasis mice) to obtain only minor improvements in the CNS phenotypes (26,27,31),

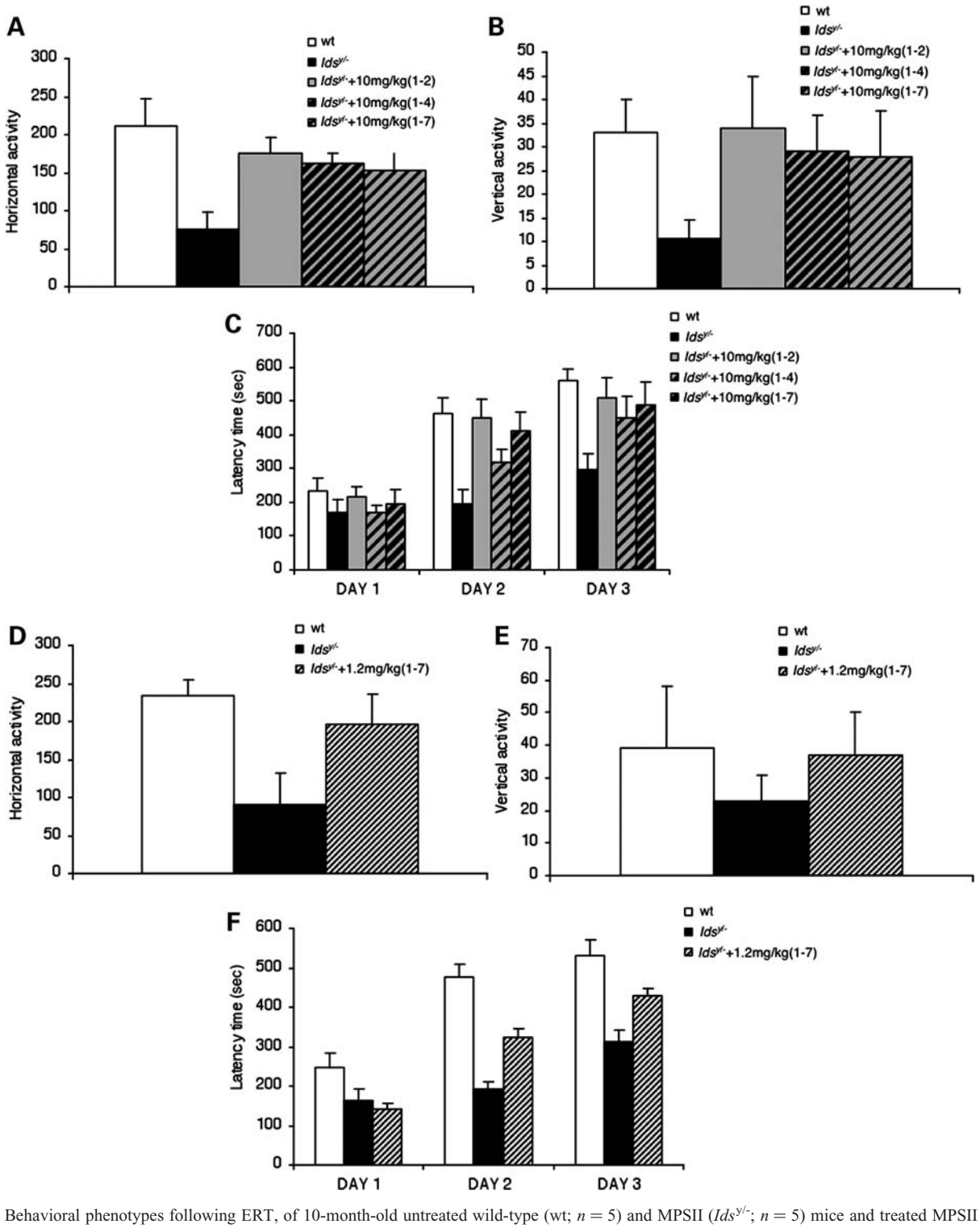

Figure 7. Behavioral phenotypes following ERT, of 10-month-old untreated wild-type (wt; $n = 5$) and MPSII (*Ids*$^{y/-}$; $n = 5$) mice and treated MPSII mice (as indicated). (**A**–**C**) Group C mice ($n = 7$) after 3 months of treatment. (**D**–**F**) Group D mice ($n = 7$) after 7 months of treatment. See text for details. Data are means $\pm$ standard deviations for the open-field test (A, B, D and E) for the number of crossings (A and D) and rearings (B and E) and for the rotarod test (C and F) for latency time. $P < 0.05$ versus untreated MPSII control (ANOVA test).

here we have a scenario in which a dose that is very close to that used already in the clinic is sufficient to improve the CNS phenotype of MPSII mice. Remarkably, a clear improvement in the disease phenotype is also seen in the 7-month-old mice when a high dose (10 mg/kg) of IDS was administered once every 7 days for 3 months, showing that even when the CNS impairment is clearly manifested, ERT can be effective to ameliorate the disease.

How is this possible? Our data clearly show that the IDS plasma clearance is very slow, which might well be the reason why we can find the IDS in the brain even with low infused doses. IDS contains N-linked glycosylation sites, and the circulating enzyme is highly sialylated (32,33). This was considered important to mask immune reactivity and to reduce receptor recapture, resulting in a high amount of circulating IDS and therefore reduced clearance. In contrast, other lysosomal enzymes currently used in ERT protocols also contain N-linked oligosaccharides; however, their clearance is much faster.

How the IDS crosses the blood–brain barrier and reaches the brain remains a mystery at present, and it will be extremely interesting to understand this further. Indeed, the stability of the IDS enzyme in the plasma leads us to conclude that it is an important parameter for the crossing of the blood–brain barrier by IDS. Whether high circulating levels of IDS are required for its delivery through receptor-mediated uptake or via different routes remains an open question.

β-glucuronidase fused to the HIV Tat peptide was shown to be taken up by absorptive endocytosis, which was mediated by binding to heparan sulfate on the cell surface (34). Similarly, the exposure of brain capillaries to high levels of circulating enzyme might lead the heparan sulfate of the BBB endothelial cells of MPSII mice to facilitate IDS delivery to the brain. Finally, we cannot exclude also an injection-dependent hydrodynamic effect, due to the high volume of IDS infused. Thus, further studies to address the mechanism of the barrier crossing will perhaps be important to modify the IDS enzyme so as to promote an increase in its uptake into the brain. Indeed, although we saw relatively low activity of the IDS enzyme in brain homogenates after these treatments, this activity appeared to be sufficient to greatly ameliorate the CNS markers and neurobehavioral symptoms in the treated mice. Importantly, we clearly obtained clearance of GAG storage in the lysosomes after IDS uptake. This is an additional important characteristic of IDS, i.e. how a low amount of this enzyme is already sufficient to ameliorate the phenotype.

In truth, however, whether these therapeutic approaches will indeed be sufficient to treat or prevent neurodegeneration in MPSII patients is difficult to predict at present. First of all, patients are currently treated when the disease is already clearly manifest, and secondly, and unfortunately, they can also show high and variable immune responses against the infused IDS (28–30). It will be important to direct future studies toward minimizing any immune response that might be mounted in the MPSII patients, perhaps also by modifying some of the epitopes of the IDS protein. As we clearly showed that the CNS lysomal storage of MPSII mice can be normalized with a little enzymatic activity, this might well happen also in the future attempts of CNS treatment of the MPSII patients. An amelioration of the CNS phenotype in the patients might be obtained if they will be treated very early and before the neurodegeneration already impaired their cognitive functions. An optimization of the ERT protocol by adjusting the IDS dose and administration timing to a level that can be beneficial for the treatment of the CNS is however needed.

In conclusion, these studies clearly show that the systemic infusion of IDS in MPSII mice is an effective treatment for the CNS phenotype, and this work now opens up hope for effective treatment and/or prevention of the CNS defects in young and adult MPSII patients.

MATERIALS AND METHODS

Animals

Female heterozygous MPSII mice were used, as described previously (11).

Blood and tissue collection

Blood (50 μl) was collected in EDTA at different times after the injections (months 1, 3, 5 and 7; T1, T3, T5 and T7) of the treated mice and the untreated MPSII ($Ids^{y/-}$) and wild-type (control) mice. Injected human IDS (Elaprase) was kindly provided by Shire Human Genetic Therapies, Inc., Cambridge, MA, USA. The blood was centrifuged at $10\,000 \times g$ for 10 min at 4°C, and the serum (supernatant) was used for enzyme assays. Tissues were collected at the end of each treatment from the treated mice and in parallel from the untreated MPSII and wild-type mice. The mice were anesthetized and sacrificed by cardiac perfusion: the left ventricle was cannulated, an incision was made in the right atrium and the mice were perfused with 40 ml of phosphate-buffered saline (PBS). The organs were collected, and half of each was fixed (for Alcian blue staining and immunohistochemistry or immunofluorescence), and the other half of each was frozen in dry ice before being processed for the IDS activity assay.

IDS activity assay

The tissues for analysis were homogenized in water. Serum and tissue protein concentrations were determined using the Bio-Rad colorimetric assay (Bio-Rad, Hercules, CA, USA). The IDS assay was performed as described previously (35): briefly, 50 μg total protein extract was incubated with 20 μl of the fluorogenic substrate, 4-methylumbelliferyl-α-iduronide-2-sulfate (Muscerdam Substrates), for 4 h at 37°C. Then, 10 μl purified α-iduronidase from rabbit liver (Muscerdam Substrates) and 40 μl McIlvain's buffer (0.4 M Na-phosphate/0.2 M Na-citrate, pH 4.5) were added to the reaction mixture, which was then incubated for an additional 24 h at 37°C. The reaction was stopped by adding carbonate stop buffer (0.5 M $NaHCO_3$/0.5 M Na_2CO_3, pH 10.7), and the fluorescence of the 4-methylumbelliferone liberated was measured using 365 nm excitation and 460 nm emission in a fluorimeter (BIO-RAD VersaFluor Fluorometer). The enzyme activities were expressed as nmol/4 h/mg protein, as calculated through the standard curve of the fluorogenic substrate, 4-methylumbelliferyl-α-iduronide (Sigma-Aldrich).

Alcian blue staining

After the perfusion of the mice with PBS, the tissues were collected and fixed in methacarn solution (30% chloroform, 60% methanol and 10% acetic acid) for 24 h at 4°C. The next day, the tissues were embedded in paraffin (Sigma-Aldrich) after their dehydration through a 70–100% ethanol gradient.

Finally, the tissues were sectioned into 7 μm thick serial sections. The tissue sections were stained with 1% Alcian blue (Sigma-Aldrich) in hydrochloric acid. The counterstaining was performed for 2 min with Nuclear-Fast red (Sigma-Aldrich).

Immunohistochemistry and immunofluorescence

Mice brains were collected after PBS perfusion and fixed with 10% neutral buffered formalin, pH 7.0, for 12 h at 4°C. Then the brains were embedded in paraffin (Sigma-Aldrich) and dehydrated through a 70–100% ethanol gradient. Immunohistochemistry and immunofluorescence analyses were performed on 7 μm thick serial sections. The specimens were incubated for 1 h with blocking solution [Tris-buffered saline, 0.2% Tween-20 (Sigma-Aldrich) and 10% normal horse serum, Vectastain Elite ABC kit] before incubation overnight with the primary antibodies.

For immunohistochemistry analyses of Lamp2 and ubiquitin of the paraffin-embedded, formalin-fixed brains, the avidin-biotin complex (ABC) method was used (Vectastain Elite ABC kit). A monoclonal rat antibody against murine Lamp2 (diluted 1:100; Santa Cruz Biotechnology, Inc., CA, USA) and a polyclonal rabbit antibody against murine ubiquitin (diluted 1:50; Abcam, Cambridge, UK) were used. Then, secondary biotinylated horse anti-rat and anti-rabbit IgG and streptavidin–biotin–peroxidase complex (Vectastain Elite ABC kit) were used for 1 h of incubation (for anti-Lamp2 and ubiquitin). The color was developed using the ABC Elite Vector Staining kit and the horseradish peroxidase substrate (Vector Laboratories, Inc., Burlingame, CA, USA). For the detection of apoptotic cells in the brain sections, TUNEL staining kits (Chemicon International) were used, according to the manufacturer's instructions.

Immunofluorescence analyses were carried out for the detection of NeuN, GFAP and CD68 (36,37) and for the co-localization signal of Lamp2-hIDS. A monoclonal mouse antibody against murine NeuN (diluted 1:200; Abcam), a monoclonal rabbit antibody against murine GFAP (diluted 1:400; Sigma-Aldrich), a monoclonal rat antibody against murine CD68 (diluted 1:250; AbD Serotec) and an antibody against human IDS (hIDS, Shire Pharmaceuticals, Boston, MA, USA) were used for the detection of co-localization signals between Lamp2-hIDS. After washing, the sections were incubated for 1 h with secondary antibodies (Molecular Probes, Invitrogen, CA, USA). Stained sections were mounted with Vectashield with DAPI (Vector Laboratories, Inc.).

Electron microscopy

The cerebellum was excised from 10-month-old treated mice and untreated MPSII and wild-type mice and fixed in 1% glutaraldehyde in 0.2 M HEPES buffer. Then small blocks of the cerebellum tissue were cut and post-fixed in uranyl acetate and in OsO_4. After dehydration through a graded series of ethanol, the tissue samples were cleared in propylene oxide, embedded in the Epoxy medium (Epon 812) and polymerized at 60°C for 72 h. From each sample, semi-thin sections were cut with a Leica EM UC6 ultramicrotome and mounted on glass slides for light microscopic inspection to identify the Purkinje and granular cell layers. Ultrathin (70 nm thick) sections of the area of interest were obtained. Electron microscopic images were acquired from thin sections using an FEI Tecnai-12 electron microscope equipped with an ULTRA VIEW CCD digital camera (FEI, Einhoven, The Netherlands). Quantification of the lysosome-like organelle dimensions was performed using the AnalySIS software (Soft Imaging Systems GmbH, Munster, Germany).

Quantitative analysis of GAG accumulation in the urine

Urine from individual mice was collected in metabolic cages at the end of each treatment and from the untreated MPSII and wild-type mice. GAG levels in the urine were determined using the dimethylmethylene-blue-based spectrophotometry of GAGs (38). These were normalized to the creatinine content. Urine creatinine was measured using Creatinine Assay kits (Quidel Corporation, San Diego, CA, USA). Absorbance was read at 490 nm. Urinary GAG was expressed as milligram GAG/milligram creatinine.

Open-field and rotarod tests

The motor and the exploratory behaviors of treated mice were assessed in an acrylic open arena, as described previously (39). The open-field test was performed (between 09:00 and 11:00 h) using the open-field apparatus (60 cm × 60 cm × 40 cm). The floor of the wooden arena was divided equally into squares marked by red lines. In this test, the treated mice and the untreated MPSII and wild-type mice were placed individually in the center of the arena and allowed to explore freely. The number of crossings (squares crossed with all paws) and rearings (rising of the front paws) was recorded during the test period of 10 min. This apparatus was cleaned with a detergent and dried after occupancy by each mouse.

The rotarod test is designed to assess the sensory motor coordination, balance, equilibrium and motor learning. The treated mice and the untreated MPSII and wild-type mice were placed on top of the rotating rod facing away from the experimenter, in the orientation opposite to that of the rod rotation. The latency times for the mice to fall from the rod were recorded automatically by the apparatus. For the first day of the test, the mice were placed on the rotating rod set at the steady slow speed of 4 rpm and trained to remain on the rod for 60 s. After this habituation trial, each mouse was tested in four trials per day, for 3 consecutive days, with an inter-trial interval of 30 min. The rotarod apparatus (Ugo Basile, Italy) accelerates gradually from 4to 40 rpm. The cut-off time was 600 s for the trials.

Statistical analyses

The statistical significance was determined for the measurements compared by the analysis of variance (ANOVA) test.

SUPPLEMENTARY MATERIAL

Supplementary Material is available at *HMG* online.

ACKNOWLEDGEMENTS

The authors thank Alicia Gómez-Yafal (Shire Human Genetic Therapies, Inc.) for her strong support and critical comments to this work for the entire duration of the project. We also would like to thank Andrea Ballabio and Giancarlo Parenti for critical comments on the manuscript. We also thank Ivan Solombrino for technical support. We would also like to acknowledge Telethon Electron Microscopy Core Facility (Grant no. GTF08001) and IGB Microscopy Facility for the assistance with the EM analysis and Anastasia V. Egorova for the EM specimen preparation.

Conflict of Interest statement. None declared.

FUNDING

This work was supported by Shire Human Genetic Therapies, Inc., by the Telethon Foundation and by the MPS Society. Funding to pay the Open Access Charge was provided by Fondazione Telethon.

REFERENCES

1. Neufeld, E.F. and Muenzer, J. (2001) The mucopolysaccharidoses. In Scriver, C.R., Beaudet, A.L., Sly, W.S. and Valle, D. (eds), *The Metabolic and Molecular Basis of Inherited Disease*. McGraw-Hill, New York, pp. 3421–3452.
2. Muenzer, J. (2004) The mucopolysaccharidoses: a heterogeneous group of disorders with variable pediatric presentations. *J. Pediatr.*, **144**, S27–S34.
3. McKusick, V.A. (1970) The relative frequency of the Hurler and Hunter syndromes. *N. Engl. J. Med.*, **283**, 853–854.
4. Meikle, P.J., Hopwood, J.J., Clague, A.E. and Carey, W.F. (1999) Prevalence of lysosomal storage disorders. *JAMA*, **281**, 249–254.
5. Young, I.D. and Harper, P.S. (1982) Incidence of Hunter's syndrome. *Hum. Genet.*, **60**, 391–392.
6. Hopwood, J.J., Bunge, S., Morris, C.P., Wilson, P.J., Steglich, C., Beck, M., Schwinger, E. and Gal, A. (1993) Molecular basis of mucopolysaccharidosis type II: mutations in the iduronate-2-sulphatase gene. *Hum. Mutat.*, **2**, 435–442.
7. Lissens, W., Seneca, S. and Liebaers, I. (1997) Molecular analysis in 23 Hunter disease families. *J. Inherit. Metab. Dis.*, **20**, 453–456.
8. Timms, K.M., Bondeson, M.L., Ansari-Lari, M.A., Lagerstedt, K., Muzny, D.M., Dugan-Rocha, S.P., Nelson, D.L., Pettersson, U. and Gibbs, R.A. (1997) Molecular and phenotypic variation in patients with severe Hunter syndrome. *Hum. Mol. Genet.*, **6**, 479–486.
9. Vafiadaki, E., Cooper, A., Heptinstall, L.E., Hatton, C.E., Thornley, M. and Wraith, J.E. (1998) Mutation analysis in 57 unrelated patients with MPS II (Hunter's disease). *Arch. Dis. Child.*, **79**, 237–241.
10. Wilson, P.J., Suthers, G.K., Callen, D.F., Baker, E., Nelson, P.V., Cooper, A., Wraith, J.E., Sutherland, G.R., Morris, C.P. and Hopwood, J.J. (1991) Frequent deletions at Xq28 indicate genetic heterogeneity in Hunter syndrome. *Hum. Genet.*, **86**, 505–508.
11. Cardone, M., Polito, V.A., Pepe, S., Mann, L., D'Azzo, A., Auricchio, A., Ballabio, A. and Cosma, M.P. (2006) Correction of Hunter syndrome in the MPSII mouse model by AAV2/8-mediated gene delivery. *Hum. Mol. Genet.*, **15**, 1225–1236.
12. Muenzer, J., Lamsa, J.C., Garcia, A., Dacosta, J., Garcia, J. and Treco, D.A. (2002) Enzyme replacement therapy in mucopolysaccharidosis type II (Hunter syndrome): a preliminary report. *Acta. Paediatr. Suppl.*, **91**, 98–99.
13. Polito, V.A. and Cosma, M.P. (2009) IDS crossing of the blood–brain barrier corrects CNS defects in MPSII mice. *Am. J. Hum. Genet.*, **85**, 296–301.
14. Barton, N.W., Brady, R.O., Dambrosia, J.M., Di Bisceglie, A.M., Doppelt, S.H., Hill, S.C., Mankin, H.J., Murray, G.J., Parker, R.I., Argoff, C.E. *et al.* (1991) Replacement therapy for inherited enzyme deficiency-macrophage-targeted glucocerebrosidase for Gaucher's disease. *N. Engl. J. Med.*, **324**, 1464–1470.
15. Weinreb, N.J., Charrow, J., Andersson, H.C., Kaplan, P., Kolodny, E.H., Mistry, P., Pastores, G., Rosenbloom, B.E., Scott, C.R., Wappner, R.S. *et al.* (2002) Effectiveness of enzyme replacement therapy in 1028 patients with type 1 Gaucher disease after 2–5 years of treatment: a report from the Gaucher Registry. *Am. J. Med.*, **113**, 112–119.
16. Schiffmann, R., Kopp, J.B., Austin, H.A. III, Sabnis, S., Moore, D.F., Weibel, T., Balow, J.E. and Brady, R.O. (2001) Enzyme replacement therapy in Fabry disease: a randomized controlled trial. *JAMA*, **285**, 2743–2749.
17. Eng, C.M., Banikazemi, M., Gordon, R.E., Goldman, M., Phelps, R., Kim, L., Gass, A., Winston, J., Dikman, S., Fallon, J.T. *et al.* (2001) A phase 1/2 clinical trial of enzyme replacement in Fabry disease: pharmacokinetic, substrate clearance, and safety studies. *Am. J. Hum. Genet.*, **68**, 711–722.
18. Eng, C.M., Guffon, N., Wilcox, W.R., Germain, D.P., Lee, P., Waldek, S., Caplan, L., Linthorst, G.E. and Desnick, R.J. (2001) Safety and efficacy of recombinant human alpha-galactosidase A replacement therapy in Fabry's disease. *N. Engl. J. Med.*, **345**, 9–16.
19. Kakkis, E.D., Muenzer, J., Tiller, G.E., Waber, L., Belmont, J., Passage, M., Izykowski, B., Phillips, J., Doroshow, R., Walot, I. *et al.* (2001) Enzyme-replacement therapy in mucopolysaccharidosis I. *N. Engl. J. Med.*, **344**, 182–188.
20. Wraith, J.E., Clarke, L.A., Beck, M., Kolodny, E.H., Pastores, G.M., Muenzer, J., Rapoport, D.M., Berger, K.I., Swiedler, S.J., Kakkis, E.D. *et al.* (2004) Enzyme replacement therapy for mucopolysaccharidosis I: a randomized, double-blinded, placebo-controlled, multinational study of recombinant human alpha-L-iduronidase (laronidase). *J. Pediatr.*, **144**, 581–588.
21. Harmatz, P., Ketteridge, D., Giugliani, R., Guffon, N., Teles, E.L., Miranda, M.C., Yu, Z.F., Swiedler, S.J. and Hopwood, J.J. (2005) Direct comparison of measures of endurance, mobility, and joint function during enzyme-replacement therapy of mucopolysaccharidosis VI (Maroteaux–Lamy syndrome): results after 48 weeks in a phase 2 open-label clinical study of recombinant human *N*-acetylgalactosamine 4-sulfatase. *Pediatrics*, **115**, 681–689.
22. Harmatz, P., Giugliani, R., Schwartz, I., Guffon, N., Teles, E.L., Miranda, M.C., Wraith, J.E., Beck, M., Arash, L., Scarpa, M. *et al.* (2006) Enzyme replacement therapy for mucopolysaccharidosis VI: a phase 3, randomized, double-blind, placebo-controlled, multinational study of recombinant human *N*-acetylgalactosamine 4-sulfatase (recombinant human arylsulfatase B or rhASB) and follow-on, open-label extension study. *J. Pediatr.*, **148**, 533–539.
23. Tanzer, F., Buyukkayhan, D., Cansu Mutlu, E. and Kalender Korkmaz, F. (2009) Enzyme replacement therapy in an infant with Pompe's disease with severe cardiomyopathy. *J. Pediatr. Endocrinol. Metab.*, **22**, 1159–1162.
24. Schuchman, E.H. (2007) The pathogenesis and treatment of acid sphingomyelinase-deficient Niemann–Pick disease. *J. Inherit. Metab. Dis.*, **30**, 654–663.
25. Roces, D.P., Lullmann-Rauch, R., Peng, J., Balducci, C., Andersson, C., Tollersrud, O., Fogh, J., Orlacchio, A., Beccari, T., Saftig, P. *et al.* (2004) Efficacy of enzyme replacement therapy in alpha-mannosidosis mice: a preclinical animal study. *Hum. Mol. Genet.*, **13**, 1979–1988.
26. Vogler, C., Levy, B., Grubb, J.H., Galvin, N., Tan, Y., Kakkis, E., Pavloff, N. and Sly, W.S. (2005) Overcoming the blood–brain barrier with high-dose enzyme replacement therapy in murine mucopolysaccharidosis VII. *Proc. Natl Acad. Sci. USA*, **102**, 14777–14782.
27. Matzner, U., Lullmann-Rauch, R., Stroobants, S., Andersson, C., Weigelt, C., Eistrup, C., Fogh, J., D'Hooge, R. and Gieselmann, V. (2009) Enzyme replacement improves ataxic gait and central nervous system histopathology in a mouse model of metachromatic leukodystrophy. *Mol. Ther.*, **17**, 600–606.
28. Muenzer, J., Wraith, J.E., Beck, M., Giugliani, R., Harmatz, P., Eng, C.M., Vellodi, A., Martin, R., Ramaswami, U., Gucsavas-Calikoglu, M. *et al.* (2006) A phase II/III clinical study of enzyme replacement therapy with idursulfase in mucopolysaccharidosis II (Hunter syndrome). *Genet. Med.*, **8**, 465–473.
29. Muenzer, J., Gucsavas-Calikoglu, M., McCandless, S.E., Schuetz, T.J. and Kimura, A. (2007) A phase I/II clinical trial of enzyme replacement therapy in mucopolysaccharidosis II (Hunter syndrome). *Mol. Genet. Metab.*, **90**, 329–337.

30. Wraith, J.E., Scarpa, M., Beck, M., Bodamer, O.A., De Meirleir, L., Guffon, N., Meldgaard Lund, A., Malm, G., Van der Ploeg, A.T. and Zeman, J. (2008) Mucopolysaccharidosis type II (Hunter syndrome): a clinical review and recommendations for treatment in the era of enzyme replacement therapy. *Eur. J. Pediatr.*, **167**, 267–277.
31. Blanz, J., Stroobants, S., Lullmann-Rauch, R., Morelle, W., Ludemann, M., D'Hooge, R., Reuterwall, H., Michalski, J.C., Fogh, J., Andersson, C. *et al.* (2008) Reversal of peripheral and central neural storage and ataxia after recombinant enzyme replacement therapy in alpha-mannosidosis mice. *Hum. Mol. Genet.*, **17**, 3437–3445.
32. Archer, I.M., Harper, P.S. and Wusteman, F.S. (1982) Multiple forms of iduronate 2-sulphate sulphatase in human tissues and body fluids. *Biochim. Biophys. Acta*, **708**, 134–140.
33. Parkinson-Lawrence, E., Turner, C., Hopwood, J. and Brooks, D. (2005) Analysis of normal and mutant iduronate-2-sulphatase conformation. *Biochem. J.*, **386**, 395–400.
34. Orii, K.O., Grubb, J.H., Vogler, C., Levy, B., Tan, Y., Markova, K., Davidson, B.L., Mao, Q., Orii, T., Kondo, N. *et al.* (2005) Defining the pathway for Tat-mediated delivery of beta-glucuronidase in cultured cells and MPS VII mice. *Mol. Ther.*, **12**, 345–352.
35. Voznyi, Y.V., Keulemans, J.L. and van Diggelen, O.P. (2001) A fluorimetric enzyme assay for the diagnosis of MPS II (Hunter disease). *J. Inherit. Metab. Dis.*, **24**, 675–680.
36. von Lukowicz, T., Hassa, P.O., Lohmann, C., Borén, J., Braunersreuther, V., Mach, F., Odermatt, B., Gersbach, M., Camici, G.G., Stähli, B.E. *et al.* (2008) PARP1 is required for adhesion molecule expression in atherogenesis. *Cardiovasc. Res.*, **78**, 158–166.
37. da Silva, R.P. and Gordon,, S. (1999) Phagocytosis stimulates alternative glycosylation of macrosialin (mouse CD68), a macrophage-specific endosomal protein. *Biochem. J.*, **338**, 687–694.
38. de Jong, J.G., Wevers, R.A., Laarakkers, C. and Poorthuis, B.J. (1989) Dimethylmethylene blue-based spectrophotometry of glycosaminoglycans in untreated urine: a rapid screening procedure for mucopolysaccharidoses. *Clin. Chem.*, **35**, 1472–1477.
39. Bronikowski, A.M., Carter, P.A., Swallow, J.G., Girard, I.A., Rhodes, J.S. and Garland, T. Jr. (2001) Open-field behavior of house mice selectively bred for high voluntary wheel-running. *Behav. Genet.,* **31**, 309–316.